Eur. Phys. J. A **15**, 463–470 (2002)
DOI 10.1140/epja/i2001-10269-9

THE EUROPEAN PHYSICAL JOURNAL A

High-spin structure of the neutron-rich odd-odd $^{106,108}_{45}$Rh and $^{110,112}_{47}$Ag isotopes

M.-G. Porquet[1,a], Ts. Venkova[2], P. Petkov[2], A. Bauchet[1], I. Deloncle[1], A. Astier[3,b], N. Buforn[3], J. Duprat[4,1], B.J.P. Gall[5], C. Gautherin[6], E. Gueorguieva[7,c], F. Hoellinger[5], T. Kutsarova[2], R. Lucas[6], M. Meyer[3], A. Minkova[7], N. Redon[3], N. Schulz[5], H. Sergolle[4], and A. Wilson[1,d]

[1] CSNSM, IN2P3/CNRS and Université Paris-Sud, F-91405 Orsay Campus, France
[2] INRNE, BAS, 1784 Sofia, Bulgaria
[3] IPNL, IN2P3/CNRS and Université Claude Bernard, F-69622 Villeurbanne, France
[4] IPN, IN2P3/CNRS and Université Paris-Sud, F-91406 Orsay, France
[5] IReS, IN2P3/CNRS and Université Louis Pasteur, F-67037 Strasbourg Cedex 2, France
[6] DAPNIA/SPhN, CEA Saclay, F-91191 Gif-sur-Yvette, France
[7] University of Sofia, Faculty of Physics, 1126 Sofia, Bulgaria

Received: 1 June 2001 / Revised version: 15 July 2002 /
Published online: 10 December 2002 –
Communicated by D. Schwalm

Abstract. The ^{106,108}Rh and ^{110,112}Ag nuclei have been produced as fission fragments following the fusion reaction ^{28}Si + ^{176}Yb at 145 MeV bombarding energy and studied with the Eurogam2 array. The yrast high-spin states of these four odd-odd nuclei, which are observed for the first time, consist of rotational bands in which the odd proton occupies the $\pi g_{9/2}$ subshell and the odd neutron the $\nu h_{11/2}$ subshell. Their behaviour as a function of spin values does not vary with the number of neutrons: as observed in the odd-N neighbouring nuclei, the motion of the odd neutron remains decoupled from the motion of the core, from $N = 61$ to $N = 65$. Moreover, the staggering observed in the yrast bands of odd-odd isotopes is strongly reduced as compared to the large values displayed by the rotational bands built on the $\pi g_{9/2}$ subshell in the odd-A Rh and Ag isotopes. The results of particle-rotor calculations indicate that this reduction is related to a change of the core deformation.

PACS. 21.60.Ev Collective models – 23.20.Lv Gamma transitions and level energies – 25.85.Ge Charged-particle-induced fission – 27.60.+j $90 \leq A \leq 149$

1 Introduction

In the neutron-rich $A \sim 100$ mass region ($40 \leq Z \leq 50$ and $N \geq 50$), several shape transitions occur and different deformations (*e.g.*, prolate, oblate, triaxial) can coexist in the same nucleus in accordance with the underlying interplay between orbitals (see for instance [1]). For $Z \geq 44$, the active orbitals, which are near the top of the $\pi g_{9/2}$ subshell, drive the nuclear shape towards oblate deformation. On the other hand, when the neutron Fermi level lies below or near the bottom of the $\nu h_{11/2}$ subshell (as for $N \sim 60$), the shape is driven to prolate deformation. These tendencies have been deduced from the features of the yrast bands observed in the odd-Z and odd-N nuclei, since they are built on these intruder orbitals, $\pi g_{9/2}$ and $\nu h_{11/2}$, respectively. One can expect that the yrast bands of the odd-odd neighbouring nuclei, involving the two intruder orbitals at the same time, would give us the opportunity to explore the result of their conflicting influence on deformation.

We report here new results obtained in the odd-odd isotopes, ^{106,108}Rh and ^{110,112}Ag. Since they lie on the neutron-rich side of the stability line, the population of their high-spin states via the usual fusion-evaporation reactions is hindered by the lack of suitable target-projectile combinations. We have chosen another method, the use of fusion-fission reactions which produce a lot of neutron-rich nuclei which can be studied at high spin thanks to the present high-resolution γ-arrays [2]. The characteris-

[a] e-mail: porquet@csnsm.in2p3.fr
[b] *Present address*: CSNSM IN2P3-CNRS and Université Paris-Sud 91405 Orsay, France.
[c] *Present address*: NAC, Faure, ZA 7131, South Africa.
[d] *Present address*: Department of Nuclear Physics, ANU, Canberra ACT 0200, Australia.

tics of the yrast bands of these four odd-odd isotopes, which are observed for the first time, suggest that they are built on the $\pi g_{9/2} \otimes \nu h_{11/2}$ configuration: they are discussed as functions of spin and neutron number. The nuclear shape associated with this configuration is discussed in the framework of an asymmetric rotor + two-quasiparticle model. Preliminary results of this work have been reported in [3,4].

2 Experimental procedures and analysis

The $^{103\text{-}109}$Rh and $^{107\text{-}113}$Ag isotopes have been produced as fission fragments of the polonium isotopes obtained in the fusion reaction ^{28}Si + ^{176}Yb at a beam energy of 145 MeV. The beam was provided by the Vivitron accelerator at Strasbourg. A 1.5 mg/cm^2 target of ^{176}Yb was used, onto which a backing of 15 mg/cm^2 Au had been evaporated in order to stop the recoiling nuclei. The prompt γ-rays were detected with the Eurogam2 array [5], consisting of 54 escape-suppressed Ge detectors. Thirty of them were large-volume coaxial detectors positioned at backward and forward angles with respect to the beam axis. The remaining 24 detectors, arranged in two rings close to 90° to the beam direction, were four-element "clover" detectors. The data were recorded in an event-by-event mode with the requirement that a minimum of five unsuppressed Ge detectors fired in prompt coincidence. A total of 540 million coincidence events were collected, out of which 135 million were three-fold, 270 million four-fold and 108 million five-fold.

The off-line analysis consisted of both γ-γ sorting and multiple-gated spectra [6]. In addition, we analysed a three-dimensional "cube" built with the software of ref. [7]. The latter technique was useful to make a fast inspection of the data, which contain γ-ray cascades emitted by about 130 fission fragments as well as by the nuclei corresponding to the strong fusion-evaporation exit channels [8,9].

The identification of transitions depopulating high-spin levels which are completely unknown, such as those of ^{106,108}Rh and ^{110,112}Ag, is based on the fact that the prompt γ-rays emitted by complementary fragments are detected in coincidence [10,2]. From our previous studies of other pairs of complementary fragments observed in this experiment [9], we have deduced that the main complementary fragment of ^{106}Rh (^{108}Rh, respectively) is ^{92}Y (^{90}Y, respectively), and the main complementary fragment of ^{110}Ag (^{112}Ag, respectively) is ^{88}Rb (^{86}Rb, respectively). Therefore new transitions depopulating high-spin states of, for instance, ^{112}Ag can be identified from gates set on transitions of ^{86}Rb [11]. Then new transitions are used for further investigations of the coincidence data.

In fission experiments, spin values can be assigned on the basis of angular-correlation results [12]. The statistics of our present data was unfortunately too poor to perform such an analysis. Therefore, spin assignments are based upon i) the already known spins of the band head states [13], ii) the assumption that in yrast decays, spin values increase with the excitation energy, iii) the analogy with the level structures of the lighter isotopes, ^{100,102,104}Rh [14] and ^{106,108}Ag [15,16].

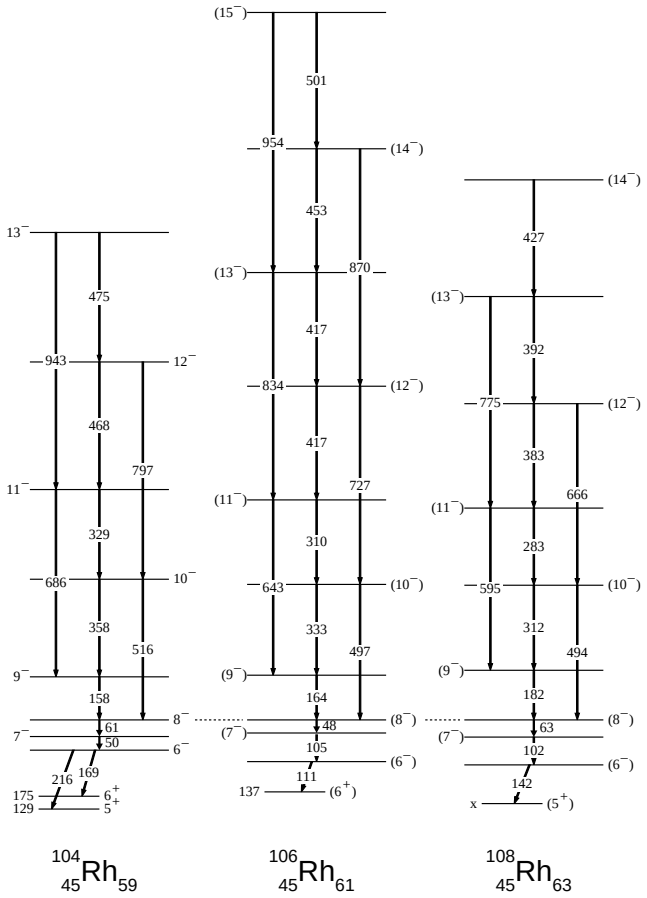

Fig. 1. High-spin level schemes of ^{104,106,108}Rh, obtained as fission fragments in the fusion reaction ^{28}Si + ^{176}Yb at 145 MeV beam energy. The energies of the (8^-) states of ^{106,108}Rh have been adjusted to the one of ^{104}Rh. The 5^+ state at 129 keV of ^{104}Rh and the (6^+) state at 137 keV of ^{106}Rh are known to be long-lived states, $T_{1/2} = 4.3$ min and 131 min, respectively [13]. The energy of the (5^+) long-lived state ($T_{1/2} = 6$ min) of ^{108}Rh is not known.

3 Experimental results

Three odd-odd Rh isotopes (^{104,106,108}Rh) have been observed in the fusion-fission reaction used in this work. High-spin structure of ^{104}Rh had been previously studied by means of the ^{100}Mo (^{7}Li, 3nγ) reaction up to an excitation energy of 2.8 MeV [14]. The level scheme observed in this work confirms the two collective structures. While the first one is built directly upon the 5^+ long-lived state ($T_{1/2} = 4.3$ min, $E = 129$ keV), the second one, which is the most populated in our reaction as it is yrast, is built on a 6^- state which decays to the positive-parity states. The latter structure is drawn in fig. 1 as it will be useful to discuss the new structures observed in the heavier masses (as explained below). Its first two transitions have

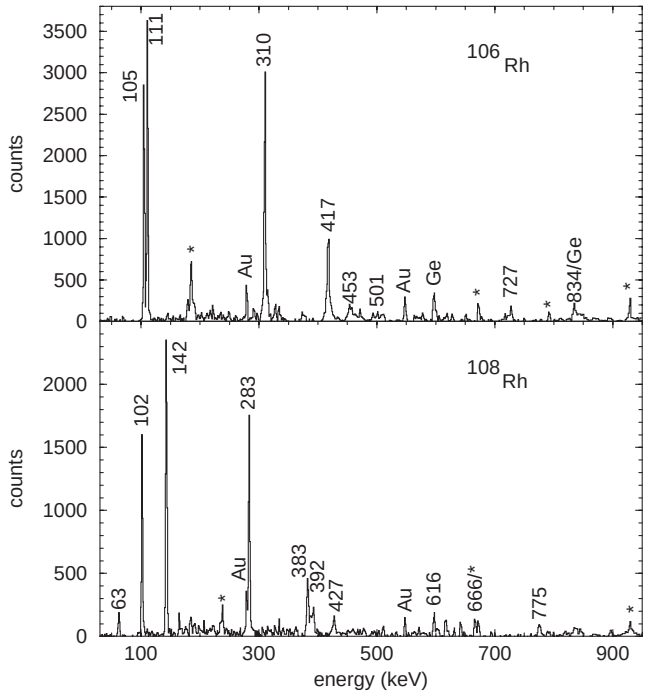

Fig. 2. Spectra of rays in double coincidence with two transitions of ^{106}Rh (164 and 333 keV) and of ^{108}Rh (182 and 312 keV). The lines marked with a star belong to their complementary fragments, ^{91,92,93}Y [18] and ^{90,91}Y [4,18], respectively.

very low energy (50 and 61 keV) and are followed by three parallel cascades. The configuration of the 6^- level, which is an isomeric state ($T_{1/2} = 47$ ns) has been assigned, from the value of its g-factor, to be $\pi g_{9/2} \otimes \nu h_{11/2}$ [17].

The present work has allowed us to identify, for the first time, the high-spin states of ^{106,108}Rh. Examples of double-gated spectra showing new transitions depopulating their yrast high-spin states are given in fig. 2. All the new transitions assigned to ^{106,108}Rh are given in table 1.

The high-spin level schemes of ^{106,108}Rh, obtained from the analysis of all the coincidence relationships observed in our data set, are shown in fig. 1. These new structures comprise firstly, three low-energy transitions (48, 105 and 111 keV in ^{106}Rh and 63, 102 and 142 keV in ^{108}Rh) and secondly, a set of six coincident gamma-rays with the corresponding cross-over transitions (having very low intensities as in the lighter isotopes), which leads to three parallel cascades. These second groups are very similar to the cascades built on the 8^- state of ^{104}Rh (see fig. 1) and in the lighter-mass Rh isotopes [19–21]. Therefore, the corresponding states of ^{106,108}Rh have been tentatively assigned as 8^-. Their decays involve three low-energy transitions, allowing the change in angular momentum of two or three units needed to reach the long-lived isomeric states of ^{106,108}Rh, (6^+) and (5^+), respectively, which are known to de-excite by beta-decays to the medium-spin states of Pd [13]. In both cases we have kept, at the bottom of the band, the same sequence of states as in ^{104}Rh: $8^- \rightarrow 7^- \rightarrow 6^-$. Indeed the yrast bands of ^{106,108}Rh isotopes are expected to consist of the same configuration, $\pi g_{9/2} \otimes \nu h_{11/2}$, as measured in ^{104}Rh [17], since our recent results have shown that the yrast structure observed in the odd-Z $^{107\text{-}109}$Rh corresponds to the $\pi g_{9/2}$ subshell [22] and the one in the odd-N ^{109,111}Pd corresponds to the $\nu h_{11/2}$ subshell [23].

It is worth noting that the first transitions of these high-spin level schemes (see fig. 1) have very low energy. The observation of such transitions strongly depends on the possibility to use a very low threshold for triggering the CFD discriminator of each channel; this could be easily performed with the VXI electronic cards of the Eurogam array [5]. Moreover, the relative efficiency has to be determined for high-fold events: this has been achieved using several cascades involving both low- and high-energy transitions with known multipolarity, in a large scale in energy (50 keV–2 MeV). From the values of gamma-ray intensities of these low-energy transitions and intensity imbal-

Table 1. Properties of the new transitions assigned to ^{106,108}Rh produced as fission fragments in the fusion reaction ^{28}Si + ^{176}Yb at a beam energy of 145 MeV. The γ-rays were detected with the Eurogam2 array, with the requirement that a minimum of five unsuppressed Ge detectors fired in prompt coincidence.

	$E_\gamma^{(a)}$ (keV)	$I_\gamma^{(a)}$	$J_i \rightarrow J_f$
^{106}Rh			
	48.1 (4)	32 (8)	$(8^-) \rightarrow (7^-)$
	104.9 (2)	111 (14)	$(7^-) \rightarrow (6^-)$
	110.7 (2)	142 (18)	$(6^-) \rightarrow (6^+)$
	164.4 (2)	100 (10)	$(9^-) \rightarrow (8^-)$
	309.6 (2)	32 (5)	$(11^-) \rightarrow (10^-)$
	333.1 (2)	57 (8)	$(10^-) \rightarrow (9^-)$
	416.9 (5)	25 (4)[b]	$(12^-) \rightarrow (11^-)$
			$(13^-) \rightarrow (12^-)$
	453.4 (2)	6 (1)	$(14^-) \rightarrow (13^-)$
	497.5 (3)	6 (1)	$(10^-) \rightarrow (8^-)$
	501.0 (5)	3 (1)	$(15^-) \rightarrow (14^-)$
	642.8 (3)	12 (2)	$(11^-) \rightarrow (9^-)$
	726.9 (4)	4 (1)	$(12^-) \rightarrow (10^-)$
	834.0 (6)	5 (1)	$(13^-) \rightarrow (11^-)$
	870 (1)	3 (1)	$(14^-) \rightarrow (12^-)$
	954 (1)	3 (1)	$(15^-) \rightarrow (13^-)$
^{108}Rh			
	62.8 (4)	43 (11)	$(8^-) \rightarrow (7^-)$
	101.6 (2)	110 (14)	$(7^-) \rightarrow (6^-)$
	142.5 (2)	140 (17)	$(6^-) \rightarrow (5^+)$
	182.1 (2)	100 (10)	$(9^-) \rightarrow (8^-)$
	283.2 (2)	33 (6)	$(11^-) \rightarrow (10^-)$
	312.2 (2)	67 (10)	$(10^-) \rightarrow (9^-)$
	382.6 (2)	22 (4)	$(12^-) \rightarrow (11^-)$
	391.6 (2)	11 (2)	$(13^-) \rightarrow (12^-)$
	427 (1)	6 (2)	$(14^-) \rightarrow (13^-)$
	494 (1)	5 (2)	$(10^-) \rightarrow (8^-)$
	595.5 (5)	8 (3)	$(11^-) \rightarrow (9^-)$
	665.8 (3)	3 (1)	$(12^-) \rightarrow (10^-)$
	774.6 (5)	7 (2)	$(13^-) \rightarrow (11^-)$

([a]) The number in parentheses is the error in the last digit.
([b]) Total intensity of the doublet.

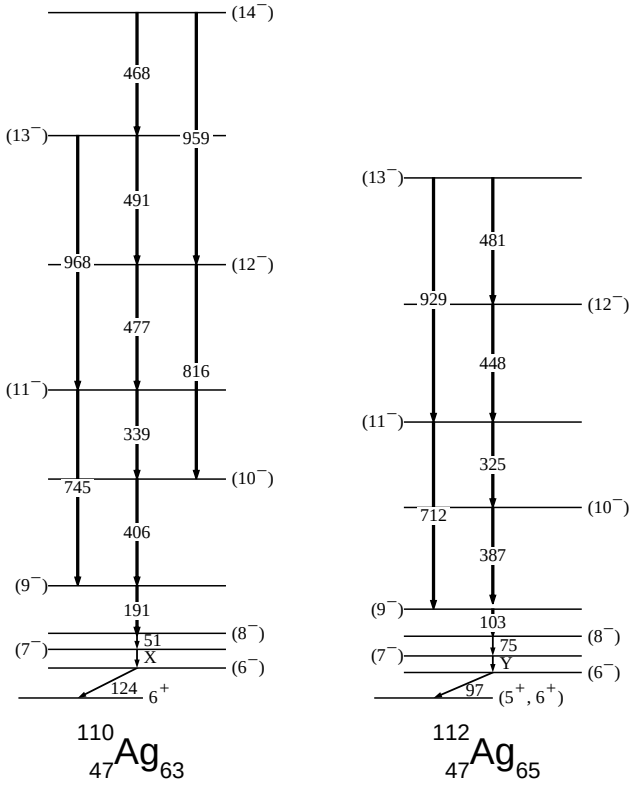

Fig. 3. High-spin level scheme of ^{110,112}Ag, obtained as fission fragments in the fusion reaction ^{28}Si + ^{176}Yb at 145 MeV beam energy. The 6^+ long-lived state ($T_{1/2} = 250$ d) of ^{110}Ag is located at 118 keV [13]. For the band head state of ^{112}Ag and for the unobserved transitions noted by X and Y, see text.

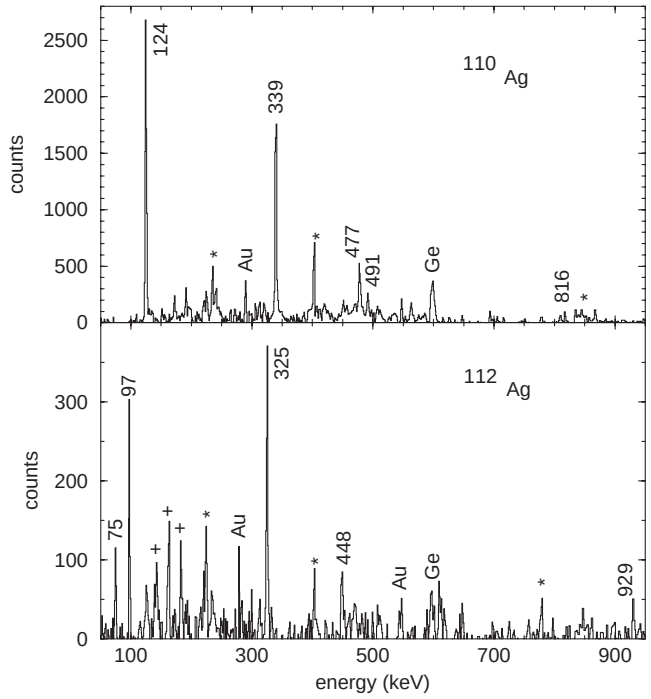

Fig. 4. Spectra of rays in double coincidence with two transitions of ^{110}Ag (191 and 406 keV) and of ^{112}Ag (103 and 387 keV). The lines marked with a star belong to their main complementary fragment, ^{88}Rb [4] and ^{86}Rb [11], respectively. Those marked with a cross have been assigned to other fission fragments emitting coincident transitions with energies very close to 103 and 387 keV.

ances, $M1$ multipolarity can be assigned to the 48 and 105 keV transitions of ^{106}Rh and to the 63 and 102 keV transitions of ^{108}Rh, while the 111 keV and 142 keV rays can be assigned as $E1$ transitions.

The high-spin level schemes of ^{110,112}Ag have been obtained, for the first time, in this work. The $_{47}$Ag isotopes are produced with lower cross-section than the $_{45}$Rh nuclei, as they are further from $Z = 42$ (which is produced with the highest yield in this symmetric fission [9]). This explains why the ^{110,112}Ag high-spin level schemes are slightly less developed (see fig. 3). Two examples of double-gated spectra showing new transitions observed in ^{110,112}Ag are given in fig. 4.

The global features of the transitions newly identified in ^{110,112}Ag from the present work (see table 2) are very similar to the ones in ^{106,108}Rh, which have been reported above, and ^{106,108}Ag [15,16]. The sole difference is the number of low-energy transitions, since only two transitions have been observed and placed at the bottom of the bands: 51 and 124 keV in ^{110}Ag, 75 and 97 keV in ^{112}Ag.

Therefore, one transition involved in each cascade $8^- \rightarrow 7^- \rightarrow 6^-$ has probably escaped from our experimental detection (they are noted by X and Y, respectively, in fig. 3). Indeed we can assume that the spin value of the band head corresponding to the configuration $\pi g_{9/2} \otimes \nu h_{11/2}$, which is $I^\pi = 6^-$ for ^{104,106,108}Ag, remains the same for ^{110,112}Ag, since there is no change in the spin values of the band head of the yrast structure of the odd-A $_{47}$Ag from $A = 103$ to $A = 113$, nor of the odd-N $_{46}$Pd from $A = 103$ to $A = 111$.

As in ^{104,106,108}Rh and ^{108}Ag [16], the high-spin level scheme of ^{110}Ag has been built upon the long-lived isomeric state, ($I^\pi = 6^+$, $T_{1/2} = 250$ d, $E_{\rm exc} = 118$ keV) already known from its beta-decay to the medium-spin states of ^{110}Cd [13]. While such a high-spin state has never been found in ^{112}Ag (probably because of the lack of production means for such an isotope which is too heavy to be produced by fusion-evaporation reaction and too light to be obtained from fission of actinides), its existence can be inferred from the de-excitation paths of the high-spin levels observed in this work and its spin value can be assigned as 5^+ or 6^+, as in the neighbouring odd-odd nuclei.

4 Discussion

The yrast states observed in the odd-odd $^{104}_{45}$Rh are built on the isomeric ($T_{1/2} = 47$ ns) 6^- state located at 345 keV above the 1^+ ground state [13,14]. As mentioned above, the configuration $\pi g_{9/2} \otimes \nu h_{11/2}$ has been assigned to this 6^- level from the value of its g-factor [17]. The proton Fermi level is located among the high-K orbitals of the $\pi g_{9/2}$ subshell, while the neutron Fermi level lies at the bottom of the $\nu h_{11/2}$ subshell. Therefore, a perpendicular

Table 2. Properties of the new transitions assigned to ^{110,112}Ag produced as fission fragments in the fusion reaction ^{28}Si + ^{176}Yb at a beam energy of 145 MeV. The γ-rays were detected with the Eurogam2 array, with the requirement that a minimum of five unsuppressed Ge detectors fired in prompt coincidence.

	$E_\gamma^{(a)}$ (keV)	$I_\gamma^{(a)}$	$J_i \rightarrow J_f$
^{110}Ag			
	51.2 (4)	25 (8)	$(8^-) \rightarrow (7^-)$
	124.5 (2)	110 (20)	$(6^-) \rightarrow 6^+$
	191.1 (2)	100 (10)	$(9^-) \rightarrow (8^-)$
	339.1 (2)	25 (3)	$(11^-) \rightarrow (10^-)$
	406.3 (2)	45 (5)	$(10^-) \rightarrow (9^-)$
	468.0 (3)	6 (2)	$(13^-) \rightarrow (14^-)$
	477.4 (2)	17 (4)	$(12^-) \rightarrow (11^-)$
	490.8 (3)	6 (2)	$(13^-) \rightarrow (12^-)$
	745.5 (3)	11 (3)	$(11^-) \rightarrow (9^-)$
	816.4 (4)	3 (1)	$(12^-) \rightarrow (10^-)$
	959 (1)	3 (1)	$(14^-) \rightarrow (12^-)$
	968.4 (5)	7 (2)	$(13^-) \rightarrow (11^-)$
^{112}Ag			
	74.6 (5)	70 (20)	$(8^-) \rightarrow (7^-)$
	97.5 (3)	120 (15)	$(6^-) \rightarrow (5^+,6^+)$
	103.5 (2)	100 (10)	$(9^-) \rightarrow (8^-)$
	324.7 (3)	26 (4)	$(11^-) \rightarrow (10^-)$
	387.0 (2)	50 (5)	$(10^-) \rightarrow (9^-)$
	448.1 (3)	19 (4)	$(12^-) \rightarrow (11^-)$
	481 (1)	6 (2)	$(13^-) \rightarrow (12^-)$
	711.8 (5)	23 (4)	$(11^-) \rightarrow (9^-)$
	929 (1)	9 (3)	$(13^-) \rightarrow (11^-)$

([a]) The number in parentheses is the error in the last digit.

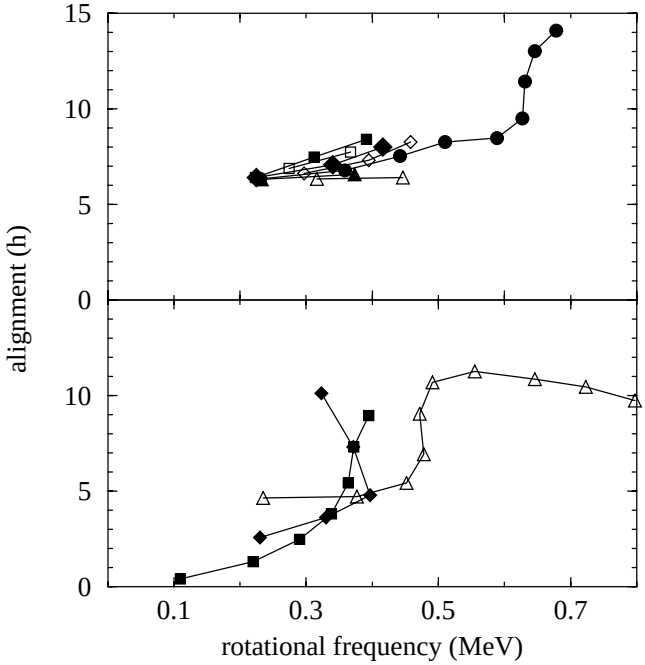

Fig. 5. Top: experimental alignments for yrast bands in ^{108}Rh (squares, this work), ^{106}Rh (diamonds, this work), ^{104}Rh (triangles up, [14] and this work), and ^{102}Rh (circles, [21]). The filled symbols correspond to positive-signature states and the empty symbols to negative-signature states. The values of Harris parameters are $\Im_0 = 9\,\hbar^2/\mathrm{MeV}$, $\Im_1 = 16\,\hbar^4/\mathrm{MeV}^3$. Bottom: experimental alignments for the ground-state band in ^{106}Ru (squares, [26]), for the $\pi g_{9/2}$ band in ^{107}Rh (diamonds, [22]), for the $\nu h_{11/2}$ band in ^{107}Pd (triangles up, [27,23]).

coupling of the angular momenta of the strongly coupled odd proton and of the decoupled odd neutron leads to a spin value $I^\pi = 6^-$ for the first level corresponding to this configuration. The peculiar behaviour of the collective structure built on such a state has been illustrated many years ago in odd-odd Tl isotopes and referred to as "semi-decoupled band" [24] or "conflicting case" [25]. The initial transition energies are small when compared to those of bands based on related configurations in neighbouring odd-A nuclei. However, as the spin increases, the cascades observed here show strong similarities with these neighbouring structures.

The new gamma-ray cascades observed in the odd-odd ^{106,108}Rh and ^{110,112}Ag isotopes also meet these criteria, giving strong support to the assignment of the same configuration as in ^{104}Rh to their yrast band observed in the present work. The behaviour of the bands as functions of the angular momentum is now discussed, focussing on Rh isotopes, since the behaviour of Ag isotopes is nearly the same.

4.1 Alignments of the yrast bands

The experimental alignments $i(\hbar)$ for the yrast bands in the odd-odd $^{102\text{-}108}$Rh are presented in fig. 5 as functions of the rotational frequency. They have been calculated following the procedure described in ref. [28] with the Harris parameters, $\Im_0 = 9\ \hbar^2/\mathrm{MeV}$, $\Im_1 = 16\ \hbar^4/\mathrm{MeV}^3$, which have been used to describe the rotational band recently observed in ^{102}Rh up to very high spin [21]. They can be compared to typical alignments observed in three neighbouring isotopes, even-even (^{106}Ru), odd-Z (^{107}Rh), and odd-N (^{107}Pd) nuclei, which are drawn in the bottom part of fig. 5. In this mass region, the first crossing observed around the frequency of 0.35 MeV in the bands built either on the ground state of the even-even nuclei or on the $\pi g_{9/2}$ state of the odd-Z nuclei is interpreted as a $(\nu h_{11/2})^2$ pair breaking. When an odd neutron occupies the $\nu h_{11/2}$ subshell, the first crossing is delayed to a frequency around 0.5 MeV, as observed in the odd-N Pd isotopes. No crossing is observed in ^{104,106,108}Rh up to a frequency of 0.45 MeV (see fig. 5); this is consistent with the blocking of the first $\nu h_{11/2}$ orbital for the configuration assigned to these yrast states, $\pi g_{9/2} \otimes \nu h_{11/2}$.

The peculiar behaviour of the alignment extracted for ^{102}Rh (drawn with solid circles in fig. 5) has to be pointed out. This is the first odd-odd nucleus in which terminating bands have been observed, implying that its shape strongly evolves with angular momentum, from collective prolate to non-collective oblate deformation [21]. Therefore, it does not exhibit the alignment of the first non-

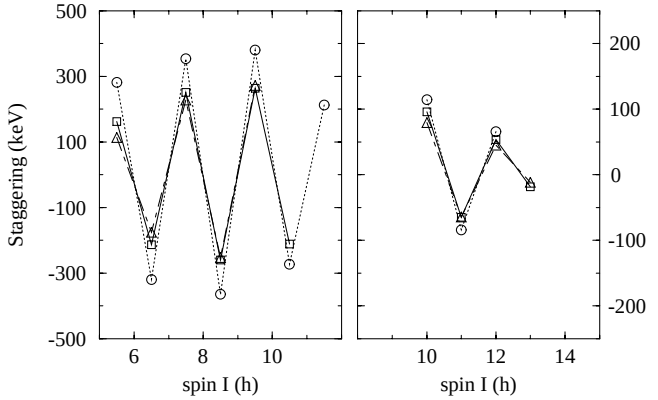

Fig. 6. Staggerings observed in the yrast bands of Rh isotopes as functions of spin values. Left: odd-A isotopes, ^{105}Rh (circles), ^{107}Rh (squares), ^{109}Rh (triangles up) ([22]). Right: odd-odd isotopes, ^{104}Rh (circles), ^{106}Rh (squares), ^{108}Rh (triangles up).

blocked pair of $\nu h_{11/2}$ quasineutrons, expected around 0.5 MeV for constant deformation of the core. The large variation of alignment occuring at 0.65 MeV is the manifestation of the rapid shape transition above the state of spin 18^-.

4.2 Staggering of the energies of yrast states

In many cases, rotational bands observed in odd and odd-odd nuclei do not display the regular structure expected from the strong-coupling hypothesis, since excited levels with one signature are shifted as compared to the ones with the other signature. The signature splitting can be evaluated from the value of the staggering defined as $S(I) = [E(I) - E(I-1)] - \frac{1}{2}\{[E(I+1) - E(I)] + [E(I-1) - E(I-2)]\}$, where $E(I)$ is the excitation energy of the state of spin I. A signature splitting is expected as far as large Coriolis mixings are involved. This is always the case at very high spin. Moreover such an effect can also be observed at the bottom of a rotational band when the Fermi level is located between two orbits coming from a high-j subshell. A triaxial deformation can also contribute to the signature splitting, as K is no longer a good quantum number.

The staggerings observed in the yrast bands of Rh isotopes as functions of spin values are drawn in fig. 6.

The values obtained in the odd-A isotopes remain almost constant as functions of spin values. Whereas the weak deformation of ^{105}Rh can explain its large signature splitting, the origin of the phenomenon in ^{107,109}Rh is different. They are more deformed but the triaxiality plays a major role [22]. As regards the odd-odd nuclei (see the right part of fig. 6), they exhibit two striking features: i) the staggering strongly decreases when the spin is increasing, ii) the signature splitting is anomalous. Indeed, the favored signature of the configuration $j_\mathrm{n} \otimes j_\mathrm{p}$ for the high-spin states of an odd-odd nucleus is expected to be $\alpha_\mathrm{f} = \frac{1}{2}\{(-1)^{j_\mathrm{p}-\frac{1}{2}} + (-1)^{j_\mathrm{n}-\frac{1}{2}}\}$ [29]. That gives $\alpha_\mathrm{f} = 0$ for the $\pi g_{9/2} \otimes \nu h_{11/2}$ configuration, whereas the positive value of the S-parameter obtained for the even-spin values means that the $\alpha = 0$ states are unfavored.

It is worth noting that observation of anomalous signature splitting is a common feature in many mass regions, $A \sim 80$ for the $\pi g_{9/2} \otimes \nu g_{9/2}$ configuration [30], $A \sim 120$ for the $\pi h_{11/2} \otimes \nu h_{11/2}$ configuration [31], $A \sim 150$ for the $\pi h_{11/2} \otimes \nu i_{13/2}$ configuration [32]. Furthermore, in almost all cases, the normal signature splitting is achieved above some spin value (depending on the nucleon numbers). This signature inversion effect has been studied in various theoretical frameworks, giving different explanations. Some of them involve the same grounds as in the odd-A cases, such as the influence of triaxial shapes or the particular locations of the two Fermi levels among the orbitals originating from high-j subshells for axial shapes. Moreover a significant residual proton-neutron interaction can also induce an anomalous signature splitting followed by signature inversion [33]. The strong decrease of the staggering values observed in the odd-odd Rh (see fig. 6) lends support to the suggestion that the inversion of the signatures does not persist for spin values greater than 14.

4.3 Particle-rotor calculations

To learn more about the nuclear shape associated with the newly established high-spin states based on the two-particle $\pi g_{9/2} \otimes \nu h_{11/2}$ configuration, we have performed particle-rotor calculations in the framework of the model presented in ref. [34]. It is an extension of the model dealing with only one odd particle [35] that we have recently used to describe the high-spin states of the odd-A ^{107}Rh [22].

The model Hamiltonian includes the rotational energy of the core, the quasiparticle energies of the odd proton (p) and neutron (n), and a residual proton-neutron interaction V_pn which has a delta-function form

$$V_\mathrm{pn} = \sqrt{8\pi^3}\Big(\frac{\hbar}{m\omega}\Big)^{\frac{3}{2}}\delta(\mathbf{r}_\mathrm{p} - \mathbf{r}_\mathrm{n})(u_0 + u_1\sigma_\mathrm{p}\cdot\sigma_\mathrm{n})\,, \qquad (1)$$

where σ is the spin operator of the particle. The core is treated as a rigid body with a fixed quadrupole deformation (ϵ, γ).

Our calculations concentrated mainly on ^{108}Rh because of its central position among the nuclei studied and the similarities between them. The deformed proton single-particles states arising within the modified harmonic-oscillator potential were obtained using the Nilsson parameters $\kappa = 0.069$ and $\mu = 0.45$ which are appropriate for the $N = 3, 4$ shells in the mass region considered [36]. For the calculation of the neutron states, the standard values [37] of the parameters κ and μ were used. They were found to correctly reproduce the low-lying band heads in the neighbouring odd-Pd nuclei.

Concerning the choice of the deformation parameters, we have firstly used the values $\epsilon = 0.3$ and $\gamma = 23°$ which had given a quite good description of the high-spin states of the odd ^{107}Rh [22], but they have proved to be unsuitable. Then the parameters ϵ and γ were varied until

a reasonable fit of the negative-parity band was obtained for the values of $\epsilon = 0.23$ and $\gamma = 11°$. The value of ϵ is in agreement with the mean deformation derived from the $B(E2, 2_1^+ \rightarrow 0_1^+)$ transition strengths in the 4 neighbouring even-even nuclei ($\epsilon \approx 0.21$). For the diagonalization of the full Hamiltonian we used a set of 6 positive-parity proton orbitals (all $g_{9/2}$ ones as well as the intruder 1/2[431] sloping down from across the $Z = 50$ shell gap) and the 4 lowest neutron orbitals arising from the $h_{11/2}$ subshell. These orbitals were found to be sufficient for the convergence of the calculations. To reproduce the band structure, we have varied the energy $E_{2_1^+}$ of the first-excited state of the even-even core and the attenuation ξ of the Coriolis interaction until the optimal values of $E_{2_1^+} = 164$ keV and $\xi = 0.6$ were adopted. Finally, we have also optimized the strength of the $V_{\rm pn}$ interaction and the best results were obtained with the values of $u_0 = -0.99$ MeV and $u_1 = -0.11$ MeV. Thereby, the ratio of u_0 and u_1 was kept fixed to 9:1 according to the considerations in ref. [38]. The standard values of the pairing strengths of the model [34] were reduced by 5% to account for the fact that both neutron and proton numbers are odd and the BCS calculation yielded $\Delta_{\rm p} = 0.883$ MeV and $\Delta_{\rm n} = 1.129$ MeV for the corresponding pairing gaps.

The results of the calculations are compared to the experimental data in fig. 7. The theoretical levels are displayed on the l.h.s. An overall agreement is observed for the moderate deformation ($\epsilon = 0.23$) and small triaxiality ($\gamma = 11°$) used to reproduce the level scheme. We note also that the $\Delta I = 1$ γ-ray transitions (of $M1$ multipolarity mainly) are predicted to dominate the cross-over $\Delta I = 2$ $E2$ transitions up to higher spins as found experimentally. However, some features are not satisfactorily described. These are the compression of the experimental levels near the band head (below the $I^\pi = 9^-$ level) and the staggering which decreases with the increase of the spin. We could not find a set of model parameters which can describe such fine details. Most probably, this failure is related to the assumption of a rigid core which underlies the model. Thus, when the triaxiality increases significantly ($11° < \gamma < 30°$) and the symmetric quadrupole deformation ϵ slightly decreases, the compression of the levels around the band head is better described. An example of such calculation is shown on the r.h.s. of fig. 7 for $\epsilon = 0.20$ and $\gamma = 23°$. Thereby, the $E_{2_1^+}$ energy of the core was set to 252 keV. However, with these parameters the description of the levels above the $I^\pi = 9^-$ is worse compared to the case of smaller triaxiality. This situation gives a hint for a possible explanation of the experimental findings, namely a quadrupole deformation and especially triaxiality which undergo some evolution with increasing spin. Such effects are predicted for ^{102}Ru on the basis of cranked Hartree-Fock-Bogoliubov calculations but not expected for heavier Ru isotopes including the $^{106\text{-}108}$Ru even-even cores of ^{108}Rh [26]. However, the $g_{9/2}$ proton and $h_{11/2}$ neutron orbitals responsible for the excitation considered in ^{108}Rh and the remaining nuclei of interest may polarise the core towards more soft and rotation sensitive shapes by exerting opposite deformation driving forces. Therefore, a rotationally induced shape evolution can be expected in these odd-odd nuclei but its detailed description requires a more advanced theoretical approach.

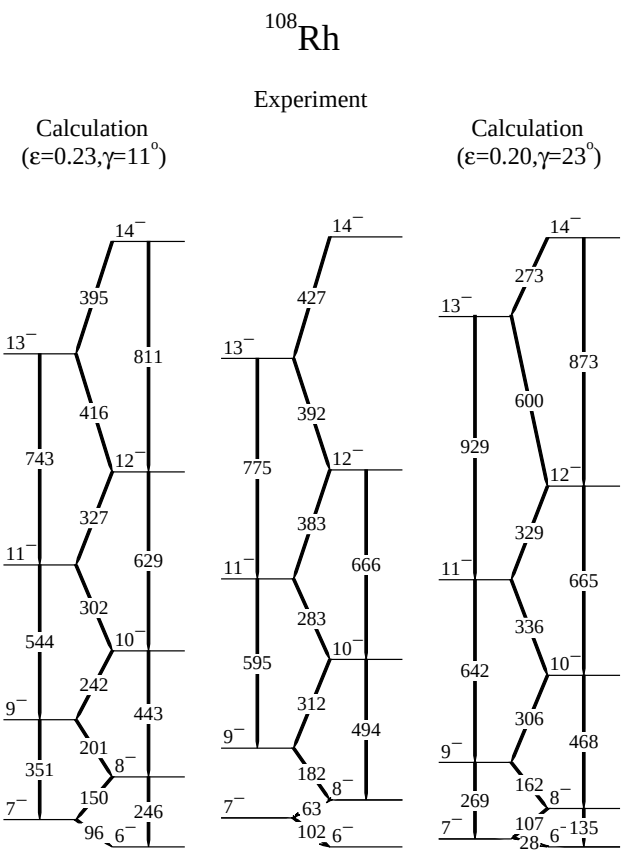

Fig. 7. Experimental $\pi g_{9/2} \otimes \nu h_{11/2}$ band structure (middle) compared to two calculations within the particle + rotor model. The calculation on the l.h.s. represents the optimal fit of the data while this on the r.h.s. was performed for the case of increased triaxiality ($\gamma = 23°$) to emphasize its effect on the levels close to the band head. The γ-ray transition energies are given in keV, while the excitation energy of the $I^\pi = 6^-$ levels is assumed to be the same in the three cases displayed. See also text.

5 Conclusion

The high efficiency of the γ-ray detector array Eurogam2 combined to an original use of a fusion-fission reaction mechanism is a very useful mean to reach high-spin states of some neutron-rich nuclei, which cannot be populated otherwise. New band stuctures have been identified in $^{106,108}_{45}$Rh and $^{110,112}_{47}$Ag isotopes. These four yrast structures are very similar. They can be interpreted in terms of an odd proton occupying orbitals from the $\pi g_{9/2}$ subshell coupled to an odd neutron occupying orbitals from the $\nu h_{11/2}$ subshell.

Their behaviour as a function of the spin value does not vary with the number of neutrons: as observed in the

odd-N neighbouring nuclei, the motion of the odd neutron remains decoupled from the motion of the core, from $N = 61$ to $N = 65$. On the other hand, the staggering observed in the yrast bands of these odd-odd isotopes is strongly reduced as compared to the large values displayed by the rotational bands built on the $\pi g_{9/2}$ subshell in the odd-A Rh and Ag isotopes. Moreover, a strong decrease of the staggering values is observed, which let suggest the occurrence of an inversion at higher-spin states. The results of the two-particle-rotor calculations indicate clearly that change of the deformation of the respective cores occurs between the odd-A Rh and odd-odd Rh isotopes. It would be extremely useful to perform lifetime measurements in order to validate these deformation changes.

The study of the yrast bands of these neutron-rich Rh and Ag has to be extended to higher spin to look for the features of the first band crossing and to the anomalous signature splitting. That would also give us information on the disappearance of the band termination phenomenon observed in ^{102}Rh when the neutron configuration space increases. Such a work is in progress.

The Eurogam project was funded jointly by IN2P3 (France) and the EPSRC (U.K.). We thank the crew of the Vivitron. We are very indebted to A. Meens for preparing the targets, G. Duchêne and D. Prévost for their help during the experiment. We also acknowledge I. Ragnarsson and P.B. Semmes for providing us with their particle-rotor codes. This work has been supported in part by the collaboration agreement Bulgarian Academy of Sciences-CNRS under contract No. 2937 and by the Bulgarian National Science Fund under contract No. Ph565.

References

1. J. Skalski, S. Mizutori, W. Nazarewicz, Nucl. Phys. A **617**, 282 (1997) and references therein.
2. M.-G. Porquet *et al.*, in *Workshop on the High Angular Momentum, Piaski, Poland (August 23-27, 1995)*, Acta Phys. Pol. **27**, 179 (1996).
3. M.-G. Porquet, in *Proceedings of the International Conference on the Nucleus: New Physics for the New Millennium, National Accelerator Centre, Faure, South Africa, January 18-22, 1999* (Kluwer Academic/Plenum Publishers, New York, 1999) p. 339.
4. M.-G. Porquet, in *Proceedings of the Second International Conference on Fission and Properties of Neutron-Rich Nuclei, St Andrews, Scotland, June 28-July 3, 1999* (World Scientific, Singapore, 2000) p. 116.
5. P.J. Nolan, F.A. Beck, D.B. Fossan, Annu. Rev. Nucl. Part. Sci. **44**, 561 (1994).
6. I. Deloncle, M.-G. Porquet, M. Dziri-Marcé, Nucl. Instrum. Methods A **357**, 150 (1995).
7. D.C. Radford, Nucl. Instrum. Methods A **361**, 296 (1995).
8. M.-G. Porquet *et al.*, in *Proceedings of the International Workshop on Research with Fission Fragments, Benediktbeuern, Germany, 28-30 Oct 1996* (World Scientific, Singapore, 1997) p. 149.
9. M.-G. Porquet *et al.*, in *International Symposium on Exotic Nuclear Shapes, Debrecen, Hungary (12-17 May 1997)*, Acta Phys. Hung., New Series, Heavy Ions Phys. **7**, 67 (1998).
10. M.A.C. Hotchkis *et al.*, Nucl. Phys. A **530**, 111 (1991).
11. G. Winter *et al.*, Phys. Rev. C **49**, 2427 (1994).
12. W. Urban *et al.*, Nucl. Instrum. Methods A **365**, 596 (1995).
13. R.B. Firestone, Table of Isotopes, 8th edition (Wiley, New York, 1996).
14. R. Duffait *et al.*, Nucl. Phys. A **454**, 143 (1986).
15. R. Popli, F.A. Rickey, L.E. Samuelson, P.C. Simms, Phys. Rev. C **23**, 1085 (1981).
16. F.R. Espinoza-Quiñones *et al.*, Phys. Rev. C **52**, 104 (1995).
17. A.M. Bizzeti-Sona *et al.*, Z. Phys. A **335**, 365 (1990).
18. M.-G. Porquet, unpublished.
19. A. Gizon *et al.*, Eur. Phys. J. A **2**, 325 (1998).
20. J. Gizon *et al.*, Phys. Rev. C **59**, R570 (1999).
21. J. Gizon *et al.*, Nucl. Phys. A **658**, 97 (1999).
22. Ts. Venkova *et al.*, Eur Phys. J. A **6**, 405 (1999).
23. T. Kutsarova *et al.*, Phys. Rev. C **58**, 1966 (1998).
24. A.J. Kreiner, Z. Phys. A **288**, 373 (1978).
25. H. Toki, H.H. Yadav, A. Faessler, Z. Phys. A **292**, 79 (1979).
26. I. Deloncle *et al.*, Eur Phys. J. A **8**, 177 (2000).
27. K.R. Pohl *et al.*, Phys. Rev. C **53**, 2682 (1996).
28. R. Bengtsson, S. Frauendorf, Nucl. Phys. A **327**, 139 (1979).
29. I. Hamamoto, Phys. Lett. B **235**, 221 (1990).
30. J. Doring, D. Ulrich, G.D. Johns, M.A. Riley, S.L. Tabor, Phys. Rev. C **59**, 71 (1999) and references therein.
31. J.F. Smith *et al.*, Phys. Lett. B **406**, 7 (1997) and references therein.
32. Y. Liu *et al.*, Phys. Rev. C **52**, 2514 (1995) and references therein.
33. P.B. Semmes, I. Ragnarsson, in *International Conference on High Spin Physics and Gamma-Soft Nuclei, Pittsburgh, September 1990* (World Scientific, Singapore, 1991) p. 500.
34. I. Ragnarsson, P. Semmes, Hyperfine Interact. **43**, 425 (1988).
35. S.E. Larsson, G. Leander, I. Ragnarson, Nucl. Phys. A **307**, 189 (1978).
36. I. Ragnarsson, S.G. Nilsson, in *Proceedings of the Colloquium on Intermediate Nuclei* (Institut de Physique Nucléaire d'Orsay, 1971) p. 112.
37. T. Bengtsson, I. Ragnarsson, Nucl. Phys. A **436**, 14 (1985).
38. W. Reviol, Phys. Rev. C **59**, 1351 (1999).